Asian Journal of Current Research in Clinical Cancer
ISSN: 3062-4444
2022, Volume 2, Issue 1, Page No: 139-152

Available online at: www.galaxypub.co/page/journals

Galaxy Publication

Galaxy Publication

Tumor-Specific MHC Class II Expression Does Not Predict Benefit from Single-Agent PD-1 Blockade in Metastatic pMMR Colorectal Cancer

Giulia J. Miller[1]*, Michael P. Gonzalez[1], Yuki L. Santos[1], Sofia Romano[1], Jun H. Smith[1]

[1]Department of Clinical Cancer Research, Faculty of Medicine, University of Oxford, Oxford, United Kingdom.

***E-mail** ✉ gmiller@hotmail.com

Received: 23 February 2022; **Revised:** 27 April 2022; **Accepted:** 28 April 2022

ABSTRACT

Effective antitumor activity of immune checkpoint inhibitors targeting the PD-(L)1 axis depends on intact interferon-γ (IFN-γ) signaling, as disruption of this pathway eliminates therapeutic benefit. While epithelial cells generally lack baseline expression of major histocompatibility complex (MHC) class II molecules, exposure to IFN-γ can induce their expression on tumor cells. This acquired tumor cell MHC class II expression has been proposed as a functional indicator of immune engagement and sensitivity to PD-(L)1 blockade. Retrospective clinical analyses across multiple malignancies have linked tumor-specific MHC class II (tsMHC-II) expression with favorable outcomes following immune checkpoint therapy. The ANICCA-Class II trial was designed to prospectively determine whether tsMHC-II expression could identify patients with proficient mismatch repair colorectal cancer (pMMR CRC) who may benefit from PD-1 inhibition. In addition, we examined whether the immunoscore–immune checkpoint (IS-IC), previously suggested as a predictive tool, could stratify outcomes in this setting. Patients with confirmed locally advanced or metastatic pMMR CRC, an ECOG performance status of 0–2, and tumor MHC class II expression greater than 1% were enrolled. Eligible participants were adults aged 18 years or older. Nivolumab was administered at a fixed dose of 480 mg every four weeks for up to 24 cycles. The primary endpoint was durable clinical benefit, defined as freedom from disease progression at the third protocol-defined radiologic assessment, approximately 27 weeks after therapy initiation. Secondary endpoints included progression-free survival and overall survival. Thirty-five patients received study treatment, with nearly two-thirds demonstrating tsMHC-II expression of at least 5%. Durable clinical benefit was achieved in three patients, yielding an observed rate of 8.6%. Bayesian modeling estimated the true durable benefit rate at 11%, with a 95% credible interval ranging from 3% to 22%, and demonstrated an extremely low likelihood that the true rate exceeded 30%. Increasing the tsMHC-II expression threshold did not enhance predictive performance for disease control. All patients who experienced durable benefit lacked liver metastases, corresponding to a benefit rate of 23.1% in patients without hepatic involvement and no observed benefit among those with liver metastases. Survival analyses showed significantly longer progression-free and overall survival in patients without liver metastases. No association was identified between high IS-IC status and treatment duration or tumor growth suppression. Prospective selection based on tumor-specific MHC class II expression does not identify patients with metastatic pMMR colorectal cancer who derive meaningful benefit from PD-1 monotherapy. Similarly, our findings do not support a predictive role for the immunoscore–immune checkpoint in this context, although the analysis is limited by sample size. The consistently poor outcomes observed in patients with liver metastases underscore the dominant immunosuppressive influence of hepatic involvement and highlight the need for therapeutic strategies capable of reversing liver-driven systemic immune tolerance.

Keywords: Colorectal cancer, PD-1 blockade, MHC class II, Metastatic pMMR

How to Cite This Article: Miller GJ, Gonzalez MP, Santos YL, Romano S, Smith JH. Tumor-Specific MHC Class II Expression Does Not Predict Benefit from Single-Agent PD-1 Blockade in Metastatic pMMR Colorectal Cancer. Asian J Curr Res Clin Cancer. 2022;2(1):139-52. https://doi.org/10.51847/sZaRWfxzIe

Introduction

Effective antitumor responses to programmed cell death protein-1 (PD-1) inhibition rely on the ability of dendritic cells to detect interferon-γ (IFN-γ) released by tumor-infiltrating T lymphocytes. Disruption of IFN-γ signaling abolishes tumor control mediated by PD-1 blockade, underscoring its central role in immune checkpoint efficacy

[1]. Consequently, multiple biomarkers have been developed to capture IFN-γ activity within the tumor microenvironment (TME), many of which correlate with response to immune checkpoint blockade (ICB). In melanoma, a defined 10-gene IFN-γ–associated signature—including IFNG, STAT1, CCR5, CXCL9, CXCL10, CXCL11, IDO1, PRF, GZMA, and the MHC class II gene HLA-DRA—effectively distinguishes responders from non-responders treated with PD-(L)1 inhibitors [2]. Broader pan-cancer analyses further demonstrate that subsets of tumors with low tumor mutational burden (TMB), yet high expression of T-cell–inflamed transcriptional programs enriched for IFN-γ–responsive genes such as PD-L1, CXCL9, STAT1, and multiple MHC class II genes, can achieve meaningful clinical benefit from ICB [3].

Under physiological conditions, epithelial cells generally lack constitutive MHC class II expression; however, exposure to IFN-γ induces transcriptional activation of CIITA via promoter IV, enabling MHC class II expression. In lung cancer, tumor-specific MHC class II (tsMHC-II) expression at levels of 5% or greater is associated with increased infiltration of both CD4+ and CD8+ T cells within the TME, as well as closer spatial interactions between immune cells and malignant cells [4]. Enhanced tsMHC-II expression also coincides with heightened T-cell activation and increased MHC class II expression on antigen-presenting immune populations, including monocytes and B cells.

Experimental models further implicate inducible tsMHC-II expression as a determinant of sensitivity to immune checkpoint therapy. In murine lung cancer systems, tumors composed of cancer cells capable of IFN-γ–induced MHC class II upregulation respond to PD-1 blockade, whereas tumors lacking this inducibility remain resistant [5]. Selective suppression of CIITA within inducible tumors diminishes responsiveness to anti-PD-1 therapy, while enforced CIITA expression in otherwise non-inducible cancer cells restores sensitivity. A substantial body of experimental evidence demonstrates that CIITA transfection enhances antitumor immune responses, with modified cancer cells functioning as surrogate antigen-presenting cells [6–10]. Clinical evidence supports these findings: in the phase III ORIENT-11 trial in lung cancer, four of the twenty genes most strongly associated with progression-free survival (PFS) in patients receiving sintilimab combined with platinum-based chemotherapy were MHC class II genes [11]. Notably, elevated MHC class II–related signatures were prognostic only in the immunotherapy combination arm and not in the chemotherapy-only group, showing stronger associations with both PFS and overall survival (OS) than MHC class I expression and across PD-L1 expression strata. CIITA expression similarly correlated with PFS exclusively in patients receiving combination therapy.

Collectively, these observations suggest that tsMHC-II expression could function as a predictive biomarker for PD-1 inhibition, a hypothesis explored in several retrospective clinical studies. In melanoma, MHC class II expression on tumor cells—often localized to the invasive tumor margin, consistent with IFN-γ exposure from infiltrating T cells—has been associated with improved outcomes [12]. Using a threshold of greater than 1% tsMHC-II positivity, patients with melanoma treated with nivolumab demonstrated higher rates of response or disease stabilization compared with tsMHC-II–negative counterparts, with any detectable tumor cell expression conferring a survival advantage. In contrast, MHC class I expression showed no predictive value. As expected, tsMHC-II positivity correlated with IFN-γ transcriptional signatures and T-cell density. These findings have been independently validated in melanoma and extended to Hodgkin lymphoma [13, 14].

The predictive relevance of tsMHC-II has also been reported in low-TMB malignancies such as triple-negative breast cancer (TNBC), which has a median TMB of approximately 1.52 mutations per megabase [15]. In PD-L1–positive TNBC, patients whose tumors exhibited tsMHC-II expression ≥5% achieved significantly higher pathological complete response (pCR) rates following neoadjuvant chemotherapy combined with durvalumab compared with those below this threshold, whereas MHC class II expression in non-tumor cells was not predictive [16]. Similar improvements in pCR have been observed in high-risk, HER2-negative breast cancer treated with neoadjuvant chemotherapy plus pembrolizumab, an effect not seen with chemotherapy alone.

Based on this collective evidence, the ANICCA-Class II trial prospectively screened patients with metastatic proficient mismatch repair colorectal cancer (pMMR CRC) for tsMHC-II expression and treated biomarker-positive individuals with nivolumab to assess whether tsMHC-II could serve as a viable selection marker for immune checkpoint therapy. This study represents, to our knowledge, both the first prospective immune checkpoint trial in any malignancy to use tumor cell MHC class II expression as an enrollment biomarker and the first biomarker-selected prospective ICB study conducted in metastatic pMMR CRC.

At present, the only biopsy-based biomarker reported to stratify outcomes for patients with metastatic pMMR CRC receiving immune checkpoint therapy is the immunoscore–immune checkpoint (IS-IC), which was retrospectively applied in the AtezoTRIBE trial [17]. The IS-IC integrates several spatial and quantitative immune

parameters, most notably CD8+ T-cell density, PD-L1–positive cell density, spatial proximity of CD8+ cells to tumor cells, and CD8+ T-cell clustering. In the randomized phase II AtezoTRIBE study, 32.6% of patients receiving atezolizumab in combination with FOLFOXIRI and bevacizumab were classified as IS-IC high. Among these patients, progression-free survival was significantly improved compared with IS-IC–low patients in the control arm (hazard ratio 0.54; 95% CI 0.31–0.94), whereas no benefit was observed in the IS-IC–low subgroup (hazard ratio 1.09). Accordingly, we also performed a retrospective assessment of IS-IC in the ANICCA-Class II cohort to determine whether this composite immune metric might predict outcomes with single-agent immune checkpoint blockade.

Materials and Methods

Study framework

ANICCA-Class II was implemented as a non-randomized, open-label, phase II investigation conducted across nine UK cancer centers (ISRCTN40245896; NCT03981146; EudraCT 2018-000318-39). Regulatory and ethical approval for the protocol (final amendment version 7.0, November 1, 2021) was obtained from the South Central–Oxford B Research Ethics Committee, in addition to site-specific institutional approvals, in accordance with applicable national and international regulations.

At trial inception, enrollment was restricted to patients whose tumors exhibited tumor-specific MHC class II (tsMHC-II) expression above 50%, with the aim of maximizing the probability of observing clinical activity. During screening, this strategy proved impractical, as such cases were exceedingly rare, likely reflecting the strong favorable prognostic association of high MHC class II expression [18]. The eligibility threshold was therefore revised to tsMHC-II expression exceeding 1%, consistent with prior melanoma data [12]. Exploratory analyses were additionally planned using a higher threshold (≥5%), previously reported to be predictive in melanoma and breast cancer [13, 16]. Coincident with this protocol modification, the nivolumab dosing schedule was changed from 240 mg administered biweekly to a flat dose of 480 mg every four weeks.

Participants

Participants were required to have a confirmed diagnosis of locally advanced or metastatic colorectal cancer with microsatellite stability and demonstrable tumor MHC class II expression greater than 1%. Eligibility was restricted to adults (≥18 years) with an Eastern Cooperative Oncology Group performance status of 0–2. Because microsatellite status was assessed by immunohistochemistry, patients are referred to as having proficient mismatch repair (pMMR) disease throughout.

All enrolled patients had exhausted standard therapeutic options and had radiographically measurable disease according to RECIST version 1.1 [19].

Pregnant or lactating individuals were excluded, and participants of reproductive potential were required to adhere to effective contraceptive measures. Written informed consent was obtained prior to any trial-related procedures. Patient registration was performed centrally via telephone by the treating investigator through the Cancer Research UK Clinical Trials Unit at the University of Birmingham.

Procedures and interventions

Nivolumab was delivered intravenously at a fixed dose of 480 mg over approximately 60 minutes (permitted variance −5 to +10 minutes) by trained clinical personnel at participating institutions. Treatment cycles were repeated every 28 days and continued on an outpatient basis for a maximum duration of two years, unless discontinued earlier because of disease progression, patient withdrawal, or unacceptable toxicity at the investigator’s discretion.

Baseline evaluations conducted within 28 days before treatment initiation included medical history, coagulation studies, contrast-enhanced CT imaging of the chest, abdomen, and pelvis, and serologic testing for hepatitis B, hepatitis C, and HIV. Additional screening assessments performed within seven days prior to enrollment comprised physical examination, body weight, vital signs, ECOG performance status documentation, review of concomitant medications, complete blood count, urinalysis, pregnancy testing where applicable, comprehensive serum chemistry, renal and thyroid function tests, and cortisol measurement.

Safety monitoring was performed at four-week intervals, with adverse events graded according to the National Cancer Institute Common Terminology Criteria for Adverse Events version 4.03 [20]. Safety follow-up continued

for up to six months after treatment discontinuation. Clinical follow-up data were collected every four weeks during the first six months and subsequently at twelve-week intervals.

Trial outcomes

The primary endpoint was durable clinical benefit (DCB), defined as the absence of radiographic disease progression at the third protocol-mandated imaging assessment following initiation of nivolumab therapy (approximately 27 weeks), or at any subsequent imaging assessment beyond this time point demonstrating continued disease control in accordance with RECIST version 1.1 [19].

Secondary efficacy endpoints included objective response (complete or partial response observed at any point during follow-up), best percentage change in the aggregate diameter of target lesions (PCSD), and time to maximal response (TTMR), calculated from treatment initiation to the imaging assessment at which an objective response was first documented. Progression-free survival (PFS) was measured from the start of study treatment to the earliest occurrence of radiographic progression or death in the absence of documented progression. Patients without progression at the time of analysis were censored at the date of their most recent evaluable imaging study. Overall survival (OS) was defined as the interval from treatment initiation to death from any cause, with surviving patients censored at their last known date alive.

Subgroup analyses based on tumor MHC class II expression (≥5% vs <5%) and the presence or absence of liver metastases were pre-specified as descriptive. However, additional post hoc inferential analyses were subsequently undertaken and are reported.

Assessment of tumor-specific MHC class II expression

Formalin-fixed, paraffin-embedded (FFPE) tumor specimens were submitted for centralized immunohistochemical (IHC) analysis at Queen Elizabeth Hospital, University Hospitals Birmingham NHS Foundation Trust, an accredited national Molecular Pathology Diagnostic Service. Central testing was used to determine both microsatellite status and MHC class II expression. Only tumors classified as proficient mismatch repair (pMMR) and demonstrating MHC class II expression in more than 1% of tumor cells were eligible to proceed to the second screening phase.

Tumor cell positivity was defined by the presence of partial or complete membranous staining and/or cytoplasmic staining of any intensity exceeding background levels. Each specimen was required to contain a minimum of 50 viable malignant cells for evaluation by a member of the central pathology team, with cases deemed equivocal undergoing independent review by a second pathologist. Immune infiltrates (including macrophages, histiocytes, and lymphocytes), stromal fibroblasts, endothelial cells, smooth muscle, and necrotic areas were excluded from scoring.

Immunostaining was performed using an anti–HLA-DR/DP/DQ antibody (Abcam ab7856, clone CR3/43) at a dilution of 1:300, with a 20-minute incubation following antigen retrieval at low pH for 20 minutes at 97°C. Staining procedures were carried out on the Dako Link 48 Autostainer using the Dako EnVision FLEX detection system. All assays were conducted in an ISO 15189–accredited clinical laboratory and validated in accordance with International Organization for Standardization requirements.

Immunoscore–immune checkpoint (IS-IC): CD8/PD-L1 dual immunohistochemistry

A dual immunohistochemistry assay was applied to quantify CD8-positive and PD-L1–positive cells within tumor regions and adjacent stromal compartments, integrating conventional IHC with digital pathology analysis. Stained slides were digitized using NanoZoomer XR and S360 scanners. The assay employed validated antibodies against CD8 (Veracyte, HD-FG-000050) and PD-L1 (Veracyte, HD-RM-000340), with staining performed on pathologist-approved FFPE sections using the Benchmark XT platform.

For each case, a pathologist calculated both the combined positive score (CPS) and the tumor proportion score (TPS) to evaluate PD-L1 expression in tumor cells and associated immune cells. Digital pathology analysis generated raw quantitative metrics for the IS-IC, including CD8+ cell density (cells/mm²), PD-L1+ cell density (cells/mm²), and multiple spatial parameters. These included CD8-centered proximity indices (percentage of CD8+ cells with at least one PD-L1+ neighbor), CD8-centered clustering indices (percentage of CD8+ cells with neighboring CD8+ cells), PD-L1–centered proximity indices (percentage of PD-L1+ cells with nearby CD8+ cells), and PD-L1–centered clustering indices (percentage of PD-L1+ cells adjacent to other PD-L1+ cells). Each spatial metric was calculated across predefined distance thresholds of 20, 40, 60, and 80 μm. As previously

reported, a maximally selected rank statistic was applied to dichotomize tumors into IS-IC HIGH or LOW categories [17].

Statistical analysis

The study employed a Bayesian adaptive design appropriate for a single-arm phase II trial. Analysis of the primary endpoint—durable clinical benefit (DCB)—used a beta-binomial conjugate framework to derive posterior distributions for the true DCB rate, incorporating a minimally informative Beta(1,1) prior. This approach enabled estimation of credible intervals and calculation of posterior probabilities to inform decision-making.

The trial was designed to detect a clinically meaningful signal, defined a priori as a true DCB rate of at least 30%, which would justify further investigation. The planned sample size was 36 treated patients, with an interim analysis scheduled after 18 patients had completed 27 weeks of follow-up. Given an anticipated prevalence of approximately 10% tsMHC-II positivity in advanced pMMR colorectal cancer, screening of roughly 360 patients was projected to achieve this target enrollment.

An independent Trial Steering Committee (TSC) conducted annual safety and oversight reviews. At the interim analysis, trial enrollment was to be halted for futility if the posterior probability that the true DCB rate was below 30% exceeded 0.90. Secondary endpoints were also considered in this assessment. At the final analysis, further research would be recommended if the posterior probability that the true DCB rate was at least 30% exceeded 0.50.

Simulation of the trial's operating characteristics indicated a 9% probability of erroneously recommending further research when the true DCB rate was 20% (analogous to a type I error) and a 91% probability of correctly recommending further research when the true DCB rate was 40% (analogous to statistical power).

All registered patients constituted the intention-to-treat population, while the per-protocol population comprised those eligible participants who received at least one treatment cycle. As these populations were identical in practice, all analyses were conducted on an intention-to-treat basis. Primary endpoint analyses were performed once all patients had accrued a minimum of 27 weeks of follow-up, with DCB reported alongside 95% credible intervals and the posterior probability that the true DCB rate met or exceeded 30%. Objective response rates were summarized as proportions with corresponding Bayesian estimates and 95% credible intervals.

Progression-free survival (PFS) and overall survival (OS) were estimated using Kaplan–Meier methods, with median survival times reported together with 95% confidence intervals; conventional confidence intervals were used because the data did not satisfy assumptions required for the preplanned exponential–inverse-gamma analysis. Best percentage change in target lesion size from baseline was visualized using waterfall plots. Time to maximal response was not reached and therefore not reported. Statistical analyses were conducted using Stata version 18.0 and R version 4.2.0.

Patient and public involvement

Patient and public involvement (PPI) was integrated throughout the study. A PPI representative contributed to trial development by reviewing patient-facing materials and providing input into protocol modifications and trial operations as a member of the Trial Management Group. Additional independent PPI representatives participated in the Trial Steering Committee, where they contributed to oversight of study conduct, safety, and recruitment.

Results and Discussion

From August 28, 2019, to September 6, 2021, a total of 464 patients with metastatic pMMR colorectal cancer who had exhausted standard treatment options were screened for tumor-specific MHC class II expression. Successful biomarker assessment was achieved in 444 patients (97.4%) **(Figure 1).** Among evaluable tumors, 13.1% (58/444) exhibited tsMHC-II expression greater than 1%, 8.8% (39/444) met the ≥5% threshold, and only 0.7% (3/444) exceeded 50% expression.

Following screening, 35 patients were enrolled and treated in the trial. Of these, 65.7% (23/35) had tumors with tsMHC-II expression of at least 5%.

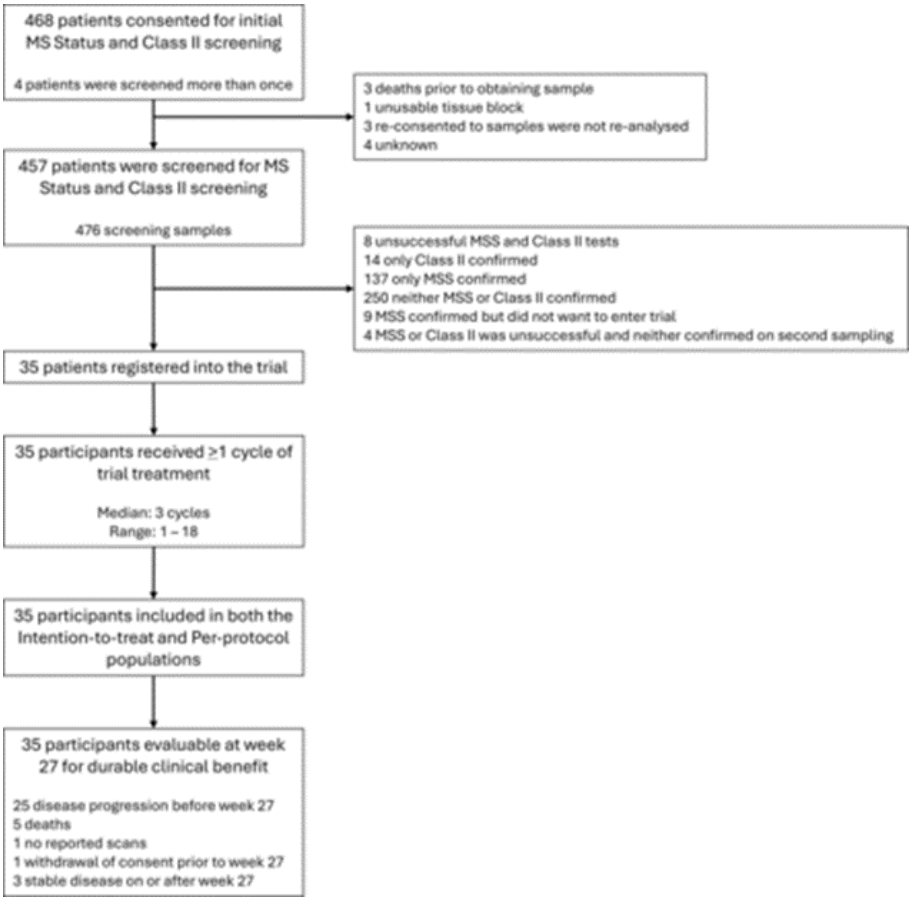

Figure 1. Flowchart illustrating screening and enrollment in the ANICCA-Class II study. The diagram summarizes patient screening and trial registration. MSS indicates microsatellite-stable disease.

Thirty-five individuals were enrolled in the trial. The cohort had a median age of 63 years, spanning from 37 to 81 years, and included a slight male predominance (54.3%, 19/35). At baseline, fewer than one-third of participants (31.4%, 11/35) had an ECOG performance status below 1, while liver involvement was common, with 62.9% (22/35) presenting with liver metastases at study entry. By the data cutoff on October 02, 2025, deaths had been recorded in 29 participants, and the median observational period across the study population was 24.4 months. No participants were removed from analysis after enrollment due to eligibility violations.

Every enrolled participant initiated nivolumab treatment and received at least one dose, resulting in identical intention-to-treat and per-protocol populations. Treatment exposure was limited overall, with a median of three administered cycles (range 1–18) and a median therapy duration of 11.9 weeks (range 3.9–77.0). Continuation on treatment differed markedly according to liver metastatic status. Only 5.7% of participants with liver metastases remained on therapy for at least 18 weeks, compared with 20.0% among those without liver involvement. At 27 weeks, these proportions declined further to 2.9% and 11.4%, respectively. Median time to treatment cessation was 9.8 weeks for participants with liver metastases and nearly double that duration (19.0 weeks) for those without. Progressive disease was cited as a reason for discontinuation in the majority of cases (80.0%, 28/35).

The prespecified interim analysis, which assessed durable clinical benefit (DCB) at approximately 27 weeks, indicated a lack of sufficient therapeutic signal, triggering early trial closure for futility. At that point, 2 of 18 evaluable participants had achieved DCB, corresponding to a 95% posterior probability that the true DCB rate was below the clinically meaningful threshold of 30%. Because recruitment continued while patients accrued the required follow-up for the primary endpoint, enrollment had reached 35 participants by the time the interim futility decision was implemented.

Final efficacy assessment confirmed the interim findings. Only 3 of 35 participants met the criteria for DCB, yielding an observed rate of 8.6%. Bayesian modeling estimated the true DCB rate at 11%, with a 95% credible interval of 3% to 22%, and demonstrated a negligible probability (0.002) that the true DCB rate reached or exceeded 30%, well below the predefined benchmark for further investigation **(Figure 2).** Applying a stricter

tumor-specific MHC class II threshold of ≥5%, which characterized 65.7% of treated participants, did not improve discrimination of clinical benefit. Within this subgroup, the DCB rate was 8.7% (2/23), and no enhancement in response, disease stabilization, or treatment duration was observed relative to the >1% eligibility criterion. These results collectively demonstrate that tumor-specific MHC class II expression, including at higher expression cut-offs, does not function as a reliable biomarker for selecting patients with advanced pMMR colorectal cancer for monotherapy with PD-1 blockade.

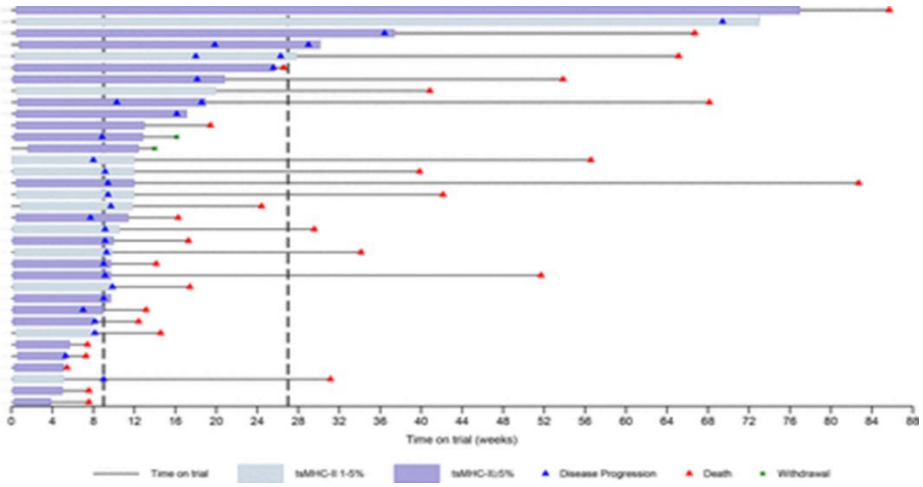

Figure 2. Duration of trial participation and clinical outcomes in relation to tumor-specific MHC class II expression.

A swimmer-style visualization depicts each participant's treatment exposure, annotated with the corresponding percentage of tsMHC-II positivity. Colored segments represent periods during which nivolumab was administered, whereas the black horizontal lines denote total follow-up duration. Vertical dashed markers indicate key protocol-defined imaging time points: approximately 9 weeks for the first on-study CT/MRI assessment and approximately 27 weeks for the third assessment, at which point participants without evidence of progression were categorized as achieving durable clinical benefit (DCB). tsMHC-II refers to tumor-specific major histocompatibility complex class II.

Durable clinical benefit was observed exclusively among participants without liver metastases at treatment initiation. Specifically, all three individuals meeting DCB criteria lacked liver involvement, corresponding to a DCB rate of 23.1% (3/13) in participants without liver metastases compared with 0% (0/22) in those with liver metastases **(Figure 3).** Within the subgroup without liver metastases, metastatic distribution was limited, with only one participant presenting lung metastases, three exhibiting peritoneal disease, and seven having involvement of sites such as adrenal gland, bone, spleen, or soft tissue.

Early disease control also differed by liver metastatic status. At the first protocol-mandated imaging assessment around week 9, stable disease was documented in nearly half of participants without liver metastases (46.2%, 6/13), whereas this outcome was considerably less frequent among those with liver involvement (18.2%, 4/22).

Across the entire study population, median progression-free survival (PFS) was short, measured at 9.0 weeks (95% CI 8.7 to 9.7), reflecting 27 progression events and seven deaths. Overall survival (OS) was similarly limited, with a median of 7.2 months (95% CI 4.0 to 11.9), during which 29 deaths occurred. Stratified analyses demonstrated significantly longer PFS and OS among participants without liver metastases compared with those with liver involvement **(Figures 4a and 4b)**.

Outcome probabilities over time further emphasized the negative prognostic impact of liver metastases. Among participants with active liver disease, the estimated 18-week PFS rate was 17.1% (95% CI 4.8% to 35.7%), and none remained under follow-up at or beyond 27 weeks. In contrast, participants without liver metastases exhibited higher PFS rates at multiple time points: 30.8% at 18 weeks (95% CI 9.5% to 55.4%), continued disease control through 27 and 36 weeks, and a 45-week PFS of 15.4% (95% CI 2.5% to 38.8%).

No participant achieved a complete or partial radiological response to nivolumab. Consequently, the predefined endpoint of time to maximal response (TTMR) was not reached, and the associated analyses were not performed **(Figure 5).**

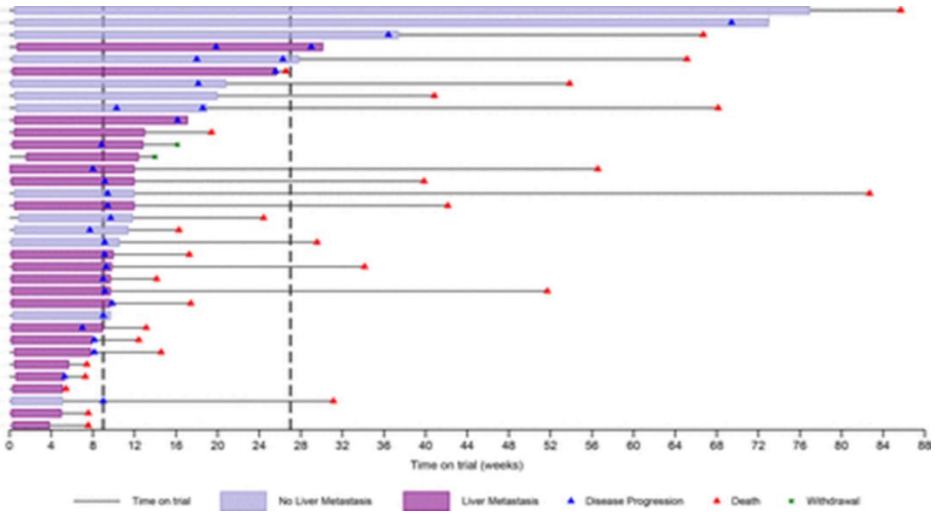

Figure 3. Trial duration and clinical outcomes stratified by liver metastatic status.

A swimmer plot illustrates individual participants' time enrolled in the study, annotated according to the presence or absence of liver metastases at baseline. Treatment exposure is depicted by colored segments, while black horizontal lines represent total follow-up time. Vertical dashed markers correspond to protocol-defined imaging milestones: approximately 9 weeks for the first on-study CT/MRI evaluation and approximately 27 weeks for the third assessment, at which participants without radiographic progression were classified as having achieved durable clinical benefit.

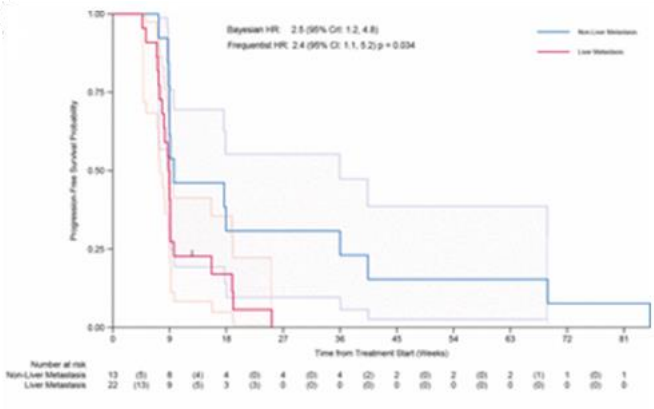

a)

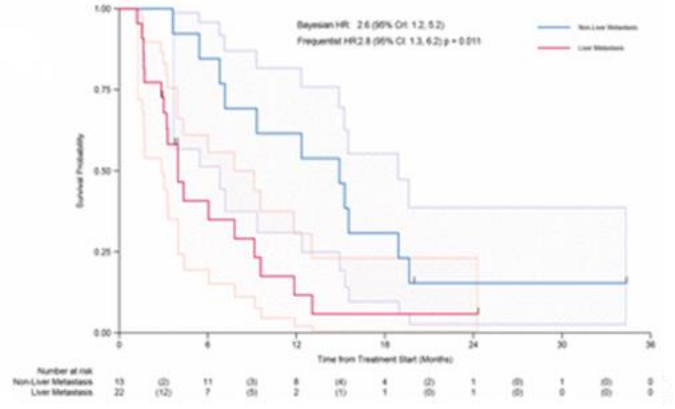

b)

Figure 4. Kaplan–Meier estimates of survival outcomes. (a) Progression-free survival (PFS) is displayed as the interval from initiation of trial therapy to the first documented radiological progression or death in the absence of prior progression. Participants alive and progression-free at the time of analysis were censored at

their most recent evaluable CT/MRI scan. (b) Overall survival (OS) is shown as the time from treatment commencement to death from any cause, with surviving participants censored at last confirmed follow-up. For both endpoints, 95% confidence intervals are provided.

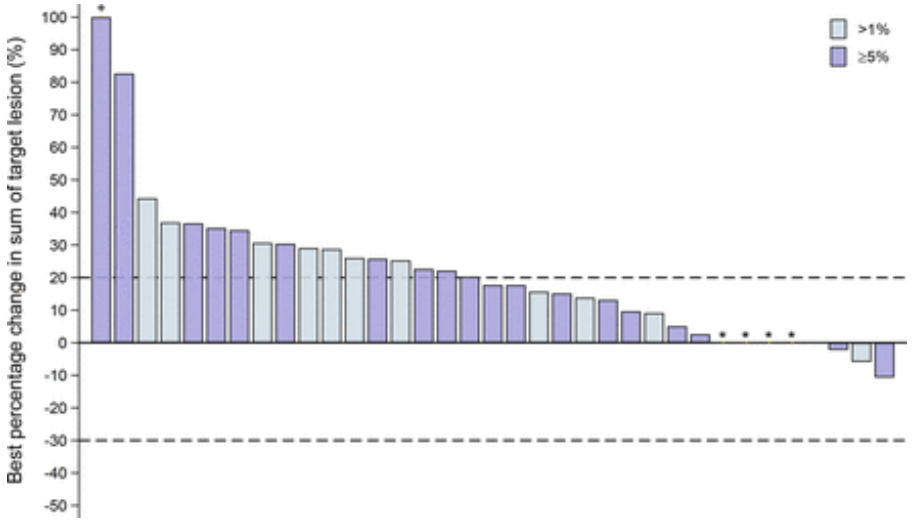

Figure 5. Maximum change in tumor burden during treatment.

At each scheduled 9-week imaging assessment, the longest diameters of all preselected target lesions were measured and summed, and percentage changes relative to baseline were calculated. The best percentage change represents the greatest reduction or, where no reduction occurred, the smallest increase observed over the entire evaluation period. Individual values are annotated with corresponding tsMHC-II expression levels. Participants marked with "+" had baseline measurements only and were classified as having progressive disease, leading to assignment of a +100% change in target lesion sum. Those indicated by "*" also had baseline-only measurements, precluding calculation of change. According to RECIST V.1.1 [19], dashed horizontal lines denote thresholds for partial response (≥30% decrease from baseline) and progressive disease (≥20% increase from baseline). tsMHC-II refers to tumor-specific major histocompatibility complex class II.

To further investigate potential biomarkers of benefit, exploratory post hoc analyses assessed the immunoscore–immune checkpoint (IS-IC). IS-IC data were available for 25 of the 35 treated participants, among whom 8 (32.0%) were classified as IS-IC HIGH, mirroring the proportion reported in the AtezoTRIBE trial [17]. Within the ANICCA-Class II cohort, tsMHC-II expression did not differ meaningfully by IS-IC category: median tsMHC-II was 4% (range 2%–30%) in IS-IC HIGH participants and 5% (range 2%–50%) in those categorized as IS-IC LOW. Similarly, the distribution of IS-IC HIGH status was comparable between participants with liver metastases and those without (33.3% vs 30%).

As expected based on IS-IC derivation, participants classified as IS-IC HIGH demonstrated significantly increased CD8+ T-cell density compared with IS-IC LOW cases ($p<0.0001$). IS-IC HIGH status was also associated with a higher density of PD-L1–positive cells across the tumor compartment ($p=0.0341$). One of the principal determinants of IS-IC, the CD8-centered proximity index at a 20 µm threshold, did not differ between groups with respect to the proportion of PD-L1+ cells neighboring CD8+ cells. However, the CD8-centered cluster index indicated a greater likelihood of CD8+ cells being located within 20 µm of another CD8+ cell in IS-IC HIGH tumors ($p=0.0491$). In addition, IS-IC HIGH tumors showed a significantly higher proportion of CD8+ cells positioned within 20 µm of PD-L1+ cells ($p<0.0017$). By contrast, PD-L1–centered clustering did not vary by IS-IC category. Collectively, these spatial and density-based immune features closely mirror those previously described in AtezoTRIBE [17].

Despite these immunological distinctions, IS-IC classification did not correlate with clinical benefit in this setting. No association was observed between IS-IC status and treatment duration, progression-free survival, or magnitude of tumor burden reduction in participants with pMMR CRC receiving nivolumab monotherapy **(Figures 6a–6c).** Although sample sizes were limited, there was no indication that IS-IC HIGH participants without liver metastases experienced enhanced benefit. Overall, inspection of swimmer and waterfall plots **(Figure 6)** suggests that IS-IC does not meaningfully stratify patients for response to single-agent PD-1 blockade in this population, in contrast

to its reported utility in the context of immune checkpoint inhibition combined with intensive chemotherapy and anti-vascular endothelial growth factor therapy [17].

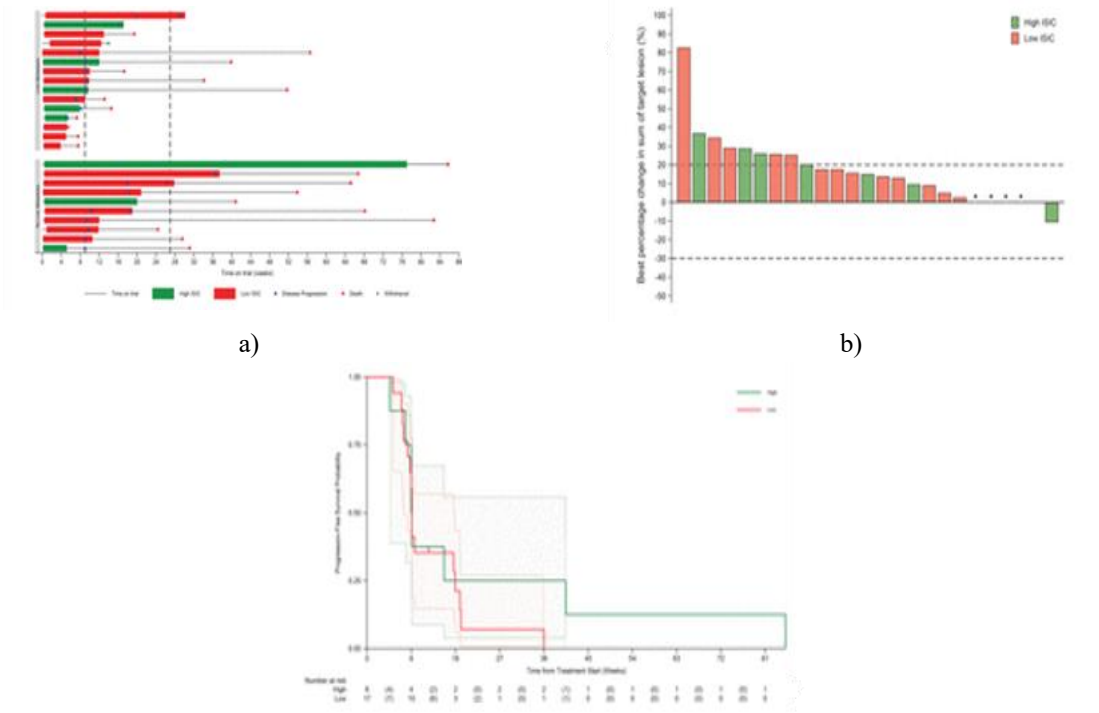

a) b)

c)

Figure 6. Clinical outcomes according to the biopsy-derived immunoscore–immune checkpoint (IS-IC). IS-IC status was successfully assigned to tumor samples from 25 of the 35 treated participants using the previously described methodology [17]. Outcomes are displayed after stratification into IS-IC HIGH and IS-IC LOW groups. (a) Individual treatment timelines are illustrated using a swimmer plot, with colored segments indicating duration of nivolumab exposure and black lines representing total follow-up. Vertical dashed markers denote approximate timing of protocol-mandated imaging, with the first assessment occurring around week 9 and the third assessment at approximately week 27. Participants without radiographic progression at the latter time point were categorized as having achieved durable clinical benefit. (b) Tumor burden dynamics are shown as the maximum percentage change in the summed longest diameters of predefined target lesions, measured at each scheduled 9-week imaging evaluation. The reported value corresponds to the largest decrease or, if no reduction occurred, the smallest increase observed during treatment. Participants indicated by an asterisk had baseline measurements only and therefore could not be assigned a change value. Dashed horizontal reference lines indicate RECIST V.1.1 thresholds for partial response (≥30% reduction from baseline) and progressive disease (≥20% increase) [19]. (c) Progression-free survival is presented as the interval from treatment initiation to the first documentation of disease progression on CT/MRI or death in the absence of prior progression. Participants alive and progression-free at the time of analysis were censored at the date of their most recent evaluable scan. Estimates include 95% confidence intervals. IS-IC denotes immunoscore–immune checkpoint.

Safety analyses demonstrated that all 35 participants who received nivolumab experienced at least one adverse event (AE) during the study. In total, 529 AEs were recorded, of which 92 were classified as grade 3 or higher. Fifteen distinct AEs occurred in at least 15% of participants; the most frequently reported were fatigue, observed in 21 of 35 individuals, and anorexia, reported in 16 of 35.

Serious adverse events were documented in 25 participants, comprising 48 events overall. Five serious AEs were attributed to study treatment, each occurring in a different participant, and included febrile neutropenia, abdominal pain, upper gastrointestinal bleeding, fatigue, and hyperbilirubinemia. No treatment-related deaths were reported. Importantly, the safety profile revealed no unexpected toxicities and no convincing evidence of hyper-progression in this biomarker-selected pMMR CRC cohort.

The ANICCA-Class II study was undertaken to determine whether a biologically plausible biomarker could identify patients with metastatic proficient mismatch repair colorectal cancer (pMMR CRC) who might experience meaningful clinical benefit from immune checkpoint blockade (ICB) administered as monotherapy. Despite strong mechanistic justification, tumor-specific MHC class II (tsMHC-II) expression failed to delineate such a population. This lack of predictive value persisted even when applying the more stringent tsMHC-II ≥5% threshold that has been associated with an immune-inflamed tumor microenvironment in lung cancer in several retrospective analyses.

A defining feature of this cohort was the high prevalence of active liver metastases (LM), a subgroup that demonstrated markedly inferior outcomes compared with participants without hepatic involvement. Screening for tsMHC-II began in September 2019. Shortly thereafter, emerging evidence suggested that the presence of LM critically modulates response to immunotherapy. In 2020, small cohort data combining regorafenib with anti-PD-1 therapy indicated improved disease stabilization predominantly among patients without LM [21]. This observation was reinforced in 2022 by an exploratory analysis of the BACCI trial, which showed higher response rates when atezolizumab was added to capecitabine and bevacizumab in patients lacking active LM [22]. More recently, compelling data published in 2024 confirmed the particularly poor efficacy of ICB in pMMR CRC patients with LM [23]. In studies combining regorafenib with nivolumab, with or without ipilimumab (R(I)N), the progression-free survival hazard ratio for patients with LM compared with those without was 3.68. Organ-specific response rates at 2 months were 0% for LM-only disease, with progressive disease observed in 93.9% of cases. By contrast, lung metastases were associated with substantially higher response rates, reaching 25% overall and 56.3% when lung disease was the sole metastatic site, compared with only 7.4% in patients harboring both lung and liver metastases. Similar reductions in ICB efficacy associated with LM have been reported in melanoma and lung cancer [24], even in settings where MHC class II expression retrospectively predicts benefit.

Although limited by sample size and dominated by patients with LM, our findings also suggest that immunoscore–immune checkpoint (IS-IC) status does not predict outcome in the context of single-agent PD-1 blockade. This represents an important negative result. In a secondary analysis of AtezoTRIBE, where approximately 75% of participants had LM, the presence of liver involvement remained strongly associated with poorer outcomes, even after adjustment for RAS and BRAF mutation status [25]. Notably, however, when anti-PD-L1 therapy was combined with intensive chemotherapy and bevacizumab, IS-IC retained its predictive capacity in patients with LM. In the present trial, the small number of participants without liver involvement precluded meaningful assessment of IS-IC performance within that subgroup.

Recently, the Society for Immunotherapy of Cancer (SITC) issued a comprehensive consensus statement outlining essential biomarkers for immunotherapy clinical trials [26]. ANICCA-Class II focused on candidate biomarkers derived from the tumor microenvironment. Within this category, SITC identifies PD-L1 immunohistochemistry (TPS or CPS) and digital pathology–based evaluation of hematoxylin and eosin features—such as tertiary lymphoid structures and tumor-infiltrating lymphocytes (TILs)—as essential. However, in a cohort exceeding 200 patients from AtezoTRIBE, concordance between TILs and IS-IC in pMMR CRC was poor [27]. Furthermore, PD-L1 status failed to predict benefit from adding atezolizumab to chemotherapy and bevacizumab in pMMR CRC. Paradoxically, among patients with high levels of tumor epithelial TILs, progression-free survival was worse in the experimental arm, with a statistically significant interaction. In contrast, patients classified as IS-IC high derived clear benefit from checkpoint blockade, with a positive interaction favoring high scores over low, underscoring the complexity of immune biomarker interpretation.

Tumor mutational burden (TMB) is listed in the SITC consensus as a key genomic biomarker. In AtezoTRIBE, IS-IC high tumors were significantly enriched for high TMB. In overall survival analyses, both IS-IC status and TMB independently predicted benefit from the addition of immune checkpoint inhibition in the pMMR subgroup [28]. However, high TMB was present in only about 5% of patients, compared with approximately 35% being IS-IC high, suggesting that reliance on TMB alone may exclude patients who could benefit from immunotherapy combined with chemotherapy and antiangiogenic therapy. Indeed, the small number of pMMR patients with high TMB limited definitive conclusions regarding its predictive utility. In non-small cell lung cancer treated with anti-PD-(L)1 agents, PD-L1 TPS has shown limited ability to predict survival outcomes, whereas IS-IC has demonstrated strong predictive performance [29]. As the SITC consensus is intended to evolve, IS-IC may eventually be recognized as an essential biomarker pending further validation, particularly if forthcoming results from the ongoing phase III trial of FOLFOXIRI/bevacizumab with or without atezolizumab confirm its utility.

A recent systematic review further corroborates the substantially higher response rates to immunotherapy in patients with pMMR CRC who do not have liver metastases [30]. Mean response rates were approximately 23% in those without LM compared with 4.7% in those with LM. For patients treated with immunotherapy alone, without antiangiogenic agents, the response rate was 14.9%. Across 28 trials included in the analysis, overall response rates ranged from 0% to 60%, while rates among patients with liver involvement ranged from 0% to 15%. These data highlight the urgent need for predictive biomarkers capable of identifying the minority of patients—approximately one in four without LM and one in twenty with LM—who may still respond to immunotherapy, especially among individuals unsuitable for intensive chemotherapy-based regimens. Although tsMHC-II and IS-IC were rationally selected based on strong retrospective evidence, neither demonstrated predictive value for ICB monotherapy in this prospective study. Importantly, this represents, to our knowledge, the first prospective evaluation of tsMHC-II as a selection biomarker for immune checkpoint blockade in any cancer. As such, these findings should motivate continued efforts to discover and validate biomarkers capable of predicting benefit from anti-PD-(L)1 therapy, with or without antiangiogenic agents. Retrospective associations between tsMHC-II and immunotherapy response in other malignancies clearly warrant prospective confirmation.
Finally, the pronounced resistance of liver metastases to ICB raises critical biological questions. Increasing evidence implicates liver-resident macrophages as key drivers of systemic T-cell suppression, thereby diminishing the efficacy of immunotherapy [31]. Single-cell RNA sequencing analyses reveal that highly immunosuppressive macrophage populations, including SPP1+ and MRC1+CCL18+ subsets, are markedly enriched in CRC liver metastases compared with primary tumors [32]. These macrophages rank among the most interactive cell types within the metastatic niche. Liver metastasis–associated tumor-associated macrophages (TAMs) express elevated levels of molecules promoting alternative polarization and exhibit reduced pro-inflammatory gene expression relative to macrophages in primary CRC. Crosstalk between SPP1+ TAMs and cancer-associated fibroblasts (CAFs) further reinforces an angiogenic, immune-excluded microenvironment through reciprocal regulation of matrisome components and signaling ligands [33].
Notably, effective neoadjuvant chemotherapy appears to remodel this immunosuppressive milieu, predominantly by altering the myeloid compartment within liver metastases [32]. Responding lesions demonstrate reductions in SPP1+ macrophages alongside increased cytotoxic T-cell infiltration, whereas non-responding metastases show expansion of immunosuppressive macrophage subsets and concomitant T-cell depletion. These findings suggest that multiagent chemotherapy regimens, such as those used in AtezoTRIBE, may be required to recondition the liver metastatic microenvironment to permit effective immune checkpoint inhibition. Alternative approaches aimed at reprogramming TAMs toward antitumor phenotypes could potentially enable successful use of single-agent ICB, with or without antiangiogenic therapy. Given the central role of Triggering Receptor Expressed on Myeloid Cells 2 (TREM2) and V-domain Ig suppressor of T-cell activation (VISTA) in the biology of alternatively polarized, metabolically reprogrammed TAMs in liver metastases [34], strategies targeting TREM2 [35] or combining anti-VISTA with immunotherapy [36] represent promising avenues. Additionally, therapeutic inhibition of CEBPβ, a transcriptional regulator critical to immunosuppressive TAM programming, merits further exploration [37].

Acknowledgments: None

Conflict of Interest: None

Financial Support: None

Ethics Statement: None

References

1. Garris CS, Arlauckas SP, Kohler RH, et al. Successful Anti-PD-1 Cancer Immunotherapy Requires T Cell-Dendritic Cell Crosstalk Involving the Cytokines IFN-γ and IL-12. Immunity. 2018;49(6):1148–61.
2. Ayers M, Lunceford J, Nebozhyn M, et al. IFN-γ-related mRNA profile predicts clinical response to PD-1 blockade. J Clin Invest. 2017;127(8):2930–40.

3. Cristescu R, Mogg R, Ayers M, et al. Pan-tumor genomic biomarkers for PD-1 checkpoint blockade-based immunotherapy. Science. 2018;362(6411):eaar3593.
4. Johnson AM, Boland JM, Wrobel J, et al. Cancer Cell-Specific Major Histocompatibility Complex II Expression as a Determinant of the Immune Infiltrate Organization and Function in the NSCLC Tumor Microenvironment. J Thorac Oncol. 2021;16(10):1694–704.
5. Johnson AM, Bullock BL, Neuwelt AJ, et al. Cancer Cell-Intrinsic Expression of MHC Class II Regulates the Immune Microenvironment and Response to Anti-PD-1 Therapy in Lung Adenocarcinoma. J Immunol. 2020;204(9):2295–307. doi:10.1136/jitc-2025-012749
6. Meazza R, Comes A, Orengo AM, et al. Tumor rejection by gene transfer of the MHC class II transactivator in murine mammary adenocarcinoma cells. Eur J Immunol. 2003;33(5):1183–92.
7. Mortara L, Castellani P, Meazza R, et al. CIITA-induced MHC class II expression in mammary adenocarcinoma leads to a Th1 polarization of the tumor microenvironment, tumor rejection, and specific antitumor memory. Clin Cancer Res. 2006;12(11):3435–43.
8. Bou Nasser Eddine F, Forlani G, Lombardo L, et al. CIITA-driven MHC class II expressing tumor cells can efficiently prime naive CD4+ TH cells in vivo and vaccinate the host against parental MHC-IInegative tumor cells. Oncoimmunology. 2017;6(12):e1261777.
9. Mortara L, Frangione V, Castellani P, et al. Irradiated CIITA-positive mammary adenocarcinoma cells act as a potent anti-tumor-preventive vaccine by inducing tumor-specific CD4+ T cell priming and CD8+ T cell effector functions. Int Immunol. 2009;21(6):655–65.
10. Frangione V, Mortara L, Castellani P, et al. CIITA-driven MHC-II positive tumor cells: preventive vaccines and superior generators of antitumor CD4+ T lymphocytes for immunotherapy. Int J Cancer. 2010;127(7):1614–24.
11. Yang Y, Sun J, Wang Z, et al. Updated Overall Survival Data and Predictive Biomarkers of Sintilimab Plus Pemetrexed and Platinum as First-Line Treatment for Locally Advanced or Metastatic Nonsquamous NSCLC in the Phase 3 ORIENT-11 Study. J Thorac Oncol. 2021;16(12):2109–20.
12. Rodig SJ, Gusenleitner D, Jackson DG, et al. MHC proteins confer differential sensitivity to CTLA-4 and PD-1 blockade in untreated metastatic melanoma. Sci Transl Med. 2018;10(450):eaar3593.
13. Johnson DB, Estrada MV, Salgado R, et al. Melanoma-specific MHC-II expression represents a tumour-autonomous phenotype and predicts response to anti-PD-1/PD-L1 therapy. Nat Commun. 2016;7:10582.
14. Roemer MGM, Redd RA, Cader FZ, et al. Major Histocompatibility Complex Class II and Programmed Death Ligand 1 Expression Predict Outcome After Programmed Death 1 Blockade in Classic Hodgkin Lymphoma. J Clin Oncol. 2018;36(9):942–50.
15. Karn T, Denkert C, Weber KE, et al. Tumor mutational burden and immune infiltration as independent predictors of response to neoadjuvant immune checkpoint inhibition in early TNBC in GeparNuevo. Ann Oncol. 2020;31(9):1216–22.
16. Gonzalez-Ericsson PI, Wulfkhule JD, Gallagher RI, et al. TumorSpecific Major Histocompatibility-II Expression Predicts Benefit to Anti-PD-1/L1 Therapy in Patients With HER2-Negative Primary Breast Cancer. Clin Cancer Res. 2021;27(18):5299–306.
17. Antoniotti C, Rossini D, Pietrantonio F, et al. Upfront FOLFOXIRI plus bevacizumab with or without atezolizumab in the treatment of patients with metastatic colorectal cancer (AtezoTRIBE): a multicentre, open-label, randomised, controlled, phase 2 trial. Lancet Oncol. 2022;23(7):876–87.
18. Løvig T, Andersen SN, Thorstensen L, et al. Strong HLA-DR expression in microsatellite stable carcinomas of the large bowel is associated with good prognosis. Br J Cancer. 2002;87(7):756–62.
19. Eisenhauer EA, Therasse P, Bogaerts J, et al. New response evaluation criteria in solid tumours: revised RECIST guideline (version 1.1). Eur J Cancer. 2009;45(15):228–47.
20. Cancer therapy evaluation program. common terminology criteria for adverse events (CTCAE) v4.03. 2010.
21. Wang C, Sandhu J, Ouyang C, et al. Clinical Response to Immunotherapy Targeting Programmed Cell Death Receptor 1/ Programmed Cell Death Ligand 1 in Patients With Treatment Resistant Microsatellite Stable Colorectal Cancer With and Without Liver Metastases. JAMA Netw Open. 2021;4(11):e2118416.
22. Mettu NB, Ou F-S, Zemla TJ, et al. Assessment of Capecitabine and Bevacizumab With or Without Atezolizumab for the Treatment of Refractory Metastatic Colorectal Cancer: A Randomized Clinical Trial. JAMA Netw Open. 2022;5(2):e2149040.

23. Fakih M, Wang C, Sandhu J, et al. Immunotherapy response in microsatellite stable metastatic colorectal cancer is influenced by site of metastases. Eur J Cancer. 2024;196:113437.
24. Tumeh PC, Hellmann MD, Hamid O, et al. Liver Metastasis and Treatment Outcome with Anti-PD-1 Monoclonal Antibody in Patients with Melanoma and NSCLC. Cancer Immunol Res. 2017;5(5):417–24.
25. Antoniotti C, Carullo M, Rossini D, et al. Liver metastases do not predict resistance to the addition of atezolizumab to firstline FOLFOXIRI plus bevacizumab in proficient MMR metastatic colorectal cancer: a secondary analysis of the AtezoTRIBE study. ESMO Open. 2025;10(2):104135.
26. Cottrell TR, Lotze MT, Ali A, et al. Society for Immunotherapy of Cancer (SITC) consensus statement on essential biomarkers for immunotherapy clinical protocols. J Immunother Cancer. 2025;13(1):e010928.
27. Moretto R, Rossini D, Catteau A, et al. Dissecting tumor lymphocyte infiltration to predict benefit from immune-checkpoint inhibitors in metastatic colorectal cancer: lessons from the AtezoT RIBE study. J Immunother Cancer. 2023;11(9):e006633.
28. Antoniotti C, Rossini D, Pietrantonio F, et al. Upfront Fluorouracil, Leucovorin, Oxaliplatin, and Irinotecan Plus Bevacizumab With or Without Atezolizumab for Patients With Metastatic Colorectal Cancer: Updated and Overall Survival Results of the ATEZOTRIBE Study. J Clin Oncol. 2024;42(22):2637–44.
29. Ghiringhelli F, Bibeau F, Greillier L, et al. Immunoscore immune checkpoint using spatial quantitative analysis of CD8 and PDL1 markers is predictive of the efficacy of anti- PD1/PD-L1 immunotherapy in non-small cell lung cancer. EBioMedicine. 2023;92:104633.
30. Beiter ER, Patel SR, Chen CT. Immunotherapy Efficacy in Mismatch Repair-Proficient Colorectal Cancer Patients With and Without Liver Metastases. J Clin Oncol. 2025.
31. Yu J, Green MD, Li S, et al. Liver metastasis restrains immunotherapy efficacy via macrophage-mediated T cell elimination. Nat Med. 2021;27(1):152–64.
32. Wu Y, Yang S, Ma J, et al. Spatiotemporal Immune Landscape of Colorectal Cancer Liver Metastasis at Single-Cell Level. Cancer Discov. 2022;12(1):134–53.
33. Sathe A, Mason K, Grimes SM, et al. Colorectal Cancer Metastases in the Liver Establish Immunosuppressive Spatial Networking between Tumor-Associated SPP1+ Macrophages and Fibroblasts. Clin Cancer Res. 2023;29(2):244–60.
34. Li S, Yu J, Huber A, et al. Metabolism drives macrophage heterogeneity in the tumor microenvironment. Cell Rep. 2022;39(5):110609.
35. Janss T, Pirson R, Rabolli V, et al. Abstract 3136: EOS-215, a first-in-class TREM2 antagonist, designed to reprogram the tumor microenvironment and overcome resistance. Cancer Res. 2025;85(14_suppl):3136.
36. Vanmeerbeek I, Naulaerts S, Sprooten J, et al. Targeting conserved TIM3(+)VISTA(+) tumor-associated macrophages overcomes resistance to cancer immunotherapy. Sci Adv. 2024;10(30):eadm8660.
37. Scuoppo C, Ramirez R, Leong SF, et al. The C/EBPβ antagonist peptide lucicebtide (ST101) induces macrophage polarization toward a pro-inflammatory phenotype and enhances anti-tumor immune responses. Front Immunol. 2025;16:1522699.